Noninvasive Depth-Resolved Optical Measurements of the Tympanic Membrane and Middle Ear for Differentiating Otitis Media

Guillermo L. Monroy, MS; Ryan L. Shelton, PhD; Ryan M. Nolan, MEng; Cac T. Nguyen, PhD;
Michael A. Novak, MD; Malcolm C. Hill, MD; Daniel T. McCormick, PhD; Stephen A. Boppart, MD, PhD

Objective/Hypothesis: In this study, optical coherence tomography (OCT) is used to noninvasively and quantitatively determine tympanic membrane (TM) thickness and the presence and thickness of any middle-ear biofilm located behind the TM. These new metrics offer the potential to differentiate normal, acute, and chronic otitis media (OM) infections in pediatric subjects.

Study Design: Case series with comparison group.

Methods: The TM thickness of 34 pediatric subjects was acquired using a custom-built, handheld OCT system following a traditional otoscopic ear exam.

Results: Overall thickness (TM and any associated biofilm) was shown to be statistically different for normal, acute, and chronic infection groups (normal-acute and normal-chronic: *P* value < 0.001; acute-chronic: *P* value = 0.0016). Almost all observed scans from the chronic group had an accompanying biofilm structure. When the thickness of the TM and biofilm were considered separately in chronic OM, the chronic TM thickness correlated with the normal group (*P* value = 0.68) yet was still distinct from the acute OM group (*P* value < 0.001), indicating that the TM in chronic OM returns to relatively normal thickness levels.

Conclusion: Identifying these physical changes in vivo provides new metrics for noninvasively and quantitatively differentiating normal, acute, and chronic OM. This new diagnostic information has the potential to assist physicians to more effectively and efficiently screen, manage, and refer patients based on quantitative data.

Key Words: Otitis media, biofilm, optical coherence tomography, pediatric, otolaryngology.

Level of Evidence: 4.

Laryngoscope, 00:000–000, 2015

INTRODUCTION

The accurate diagnosis of otitis media (OM) lies in navigating the numerous confounding and qualitative factors that may present during an exam, including patient history, physical exam, prior antibiotic prescription, swelling and/or otalgia of the tympanic membrane (TM), and

overall presentation of the infection.[1] During patient examinations, most diagnostic parameters are based on physical characteristics of the TM viewed from the ear canal, including but not limited to coloration, transparency, injection, and the presence of an effusion. The proper collection and interpretation of these qualitative parameters varies not only with illumination and observation but also with the experience of the physician.[1] The resulting sensitivity and specificity for diagnosing OM using a traditional otoscope exam has been reported to be 70%.[2] Due to this variability and subjectivity, a wide range of interpretations and diagnoses result, even among experienced physicians. Ultimately, it is important to ensure an accurate diagnosis because the specific treatment course differs among the wide range of presentations of OM. Acute cases may require close observation by the physician at subsequent follow-up visits or a prescribed antibiotic course. Similarly, chronic cases may require a different, stronger, or longer antibiotic course. Additionally, they may eventually require more invasive surgical intervention, depending on the current needs of the patient and state of the infection. Enacting a treatment plan with insufficient knowledge of the infection or an incorrect hypothesis could lead to administering a less effective treatment plan.

Other techniques used to more accurately diagnose OM and OM-related infections noninvasively have accuracies similar to a traditional otoscope exam, such as acoustic

reflectometry (sensitivity: 63.6%; specificity: 79.7%) and tympanometry (sensitivity: 86.9%; specificity: 71.7%),[3] but are still typically recommended to be used in conjunction with a traditional otoscope for diagnosis. Although the use of pneumatic otoscopy increases the diagnostic accuracy (sensitivity: +12%; specificity: +18%) when used alongside a traditional otoscope exam,[4] 25% to 50% of physicians do not utilize pneumatic otoscopy as part of their normal patient exam; 43% of pneumatic exams are performed or interpreted incorrectly without proper training.[5] Removing sufficient cerumen from the ear canal and obtaining a proper seal are the primary challenges for collecting accurate data using these techniques, which then must also be interpreted correctly. The difficulty in diagnosing and treating OM leads to a high rate of myringotomy procedures with tympanostomy tube placement, which is one of the most commonly performed surgical procedures under general anesthesia for young children.[6] The prevalence of OM leads to high direct and indirect health-care costs, estimated at approximately $3 billion nationwide.[7,8]

Otoscope designs and their technology have not significantly improved since the inception of this instrument, being little more than a device for the illumination and magnification of the surface of tissue. There is a strong need for a new, modern, diagnostic tool to better diagnose OM infections in children, especially considering the increasing evidence regarding the role of biofilms in the OM infection process.[9,10] Biofilms are aggregates of bacteria that have collectively formed an extracellular polymeric matrix in response to the surrounding environment.[11,12] These structures confer a significant increase in antibiotic resistance of approximately 1,000-fold when compared to the resistance of free-floating planktonic bacteria,[11] provide additional evasive mechanisms from the host immune system,[13] and likely serve as a reservoir for seeding recurrent infections. The presence of biofilms in the middle ear and their link to chronic OM in humans was first established in a chinchilla animal model[14] and then later in a human study in 2006.[15] Related work has shown that biofilms also inhabit the adenoids[16–19] and sinuses.[20,21] The complex role that biofilms play in upper respiratory infections in the sinuses, middle ear, and oropharynx is not yet well understood, largely due to the fact that they are difficult to observe and track in vivo.

Optical coherence tomography (OCT) has been used in previous studies to investigate and observe the structure and dynamics of the ear, both ex vivo and in vivo.[22,23] Although some recent studies have been performed in surgical settings,[24] previous investigations in humans have largely been restricted to ex vivo tissue studies[25,26] due to the technical difficulties of imaging the ear in vivo, including developing an appropriate beam-delivery system. This clinical study is driven by our previous body of work for which we first imaged in vitro biofilms with OCT to understand their microstructure and growth over time.[27] In a subsequent preclinical study, middle-ear infections were induced and imaged in a rat model,[28] which showed visible biofilm-like structures affixed to the TM. The presence of a middle-ear biofilm was later directly correlated with histological findings.[29] Following the construction of a handheld OCT scanner and portable system for clinical applications,[30,31] in vivo OCT imaging of the TM and middle-ear biofilms was demonstrated in a clinical study involving adult human subjects with or without chronic OM.[30–32]

Collectively, this body of work helped established the link between recurrent or chronic OM and biofilms in the middle ear and demonstrated that a noninvasive, real-time, OCT image of the TM can be utilized to assess the presence of a biofilm that may develop behind the TM in adult patients with chronic OM. In this study, we target the pediatric population for whom OM is most common. OCT is used to determine the thickness of the TM as well as the presence of any middle-ear biofilm located behind the TM. These results are investigated as potential new image-based metrics to differentiate normal, acute, and chronic infection states in pediatric subjects.

MATERIALS AND METHODS

This study randomly samples the outpatient pediatric population of Champaign–Urbana, Illinois, visiting Carle Foundation Hospital either at the otolaryngology specialist clinic or the primary care clinic. In total, 34 pediatric subjects were recruited for this study. Proper informed consent was acquired for all participants following institutional review board (IRB) protocols approved by the University of Illinois at Urbana–Champaign and Carle Foundation Hospital. Inclusion into one of the three subgroups (normal, acute OM, chronic OM) was based on the clinical presentation of the infection as determined by the physician's otoscopic assessment, following the recommendations outlined by the American Academy of Pediatricians in *The Diagnosis and Management of Acute Otitis Media*.[1] Generally, acute cases are defined as physical findings of effusion, pus, and/or erythema with accompanying fever or pain. Chronic cases usually present multiple episodes of infection in a 6-month time period, and/or a persistent effusion for greater than 3 months. Subjects were excluded from this study if they were 18 years of age or older to ensure a focus on OM in the pediatric population, or if the subjects' temperament and/or discomfort prohibited imaging with the handheld device. There were no gender restrictions.

A portable custom-built OCT system with a handheld scanner (Fig. 1) was used for this study, and is described in detail elsewhere.[30] The system utilized a broadband light source with a central wavelength of 830 nm, and it was capable of resolving tissue microstructure with 4-micron axial and 15-micron transverse resolution in cross-sectional images processed and displayed at rates of up to 70 frames per second—each frame consisting of 1,000 columns (A-scans).[30] Higher-resolution color surface images of each TM were collected with a commercial, digital video otoscope for documentation of the physician's diagnostic criteria.

Research image and data collection for each human subject in this study followed the regularly scheduled standard-of-care medical examination. This served to not only prevent any interruption or deviation in patient care, but also to provide the physician an opportunity to formulate an unbiased diagnostic opinion that was solely based on following the current gold standard of care. Subjects were then consented and scanned with the handheld OCT system, which added on average no more than 5 minutes to the exam visit time.

Average TM-thickness values were calculated from three representative locations for each cross-sectional OCT image. An

Fig. 1. Portable imaging system. The handheld probe has a standard ear speculum attachment mount and an internally integrated camera. The system can simultaneously collect both en face video images and cross-sectional depth-resolved OCT images of the TM and display them on the system monitor or the integrated screen on the back of the handheld probe. OCT = optical coherence tomography; TM = tympanic membrane.

index of refraction of n = 1.44 was used in this calculation, which has been shown to be the average index of refraction across the human TM in ex vivo specimens.[26] If the TM was angled in the image, its geometry was mathematically accounted for in the thickness measurements. To investigate the statistical significance of these measurements, a two-sided Welch's t test was performed to compare infection groups. A traditional Student t test was not used because it was not known if each TM thickness group had equal variance. Each grouping was considered by comparing normal-acute, acute-chronic, and normal-chronic statistics. An open-source statistical computational software package (R, The R Foundation for Statistical

Computing) was used to facilitate these calculations, which were later verified manually.

RESULTS

Representative OCT data from this study, highlighting normal ear findings, acute OM, and chronic OM pathologies—along with representative otoscopic TM video still images—are shown in Figure 2. Representative cross-sectional OCT images (Fig. 2A–C) and video still surface images (Fig. 2D–F) emphasize the different
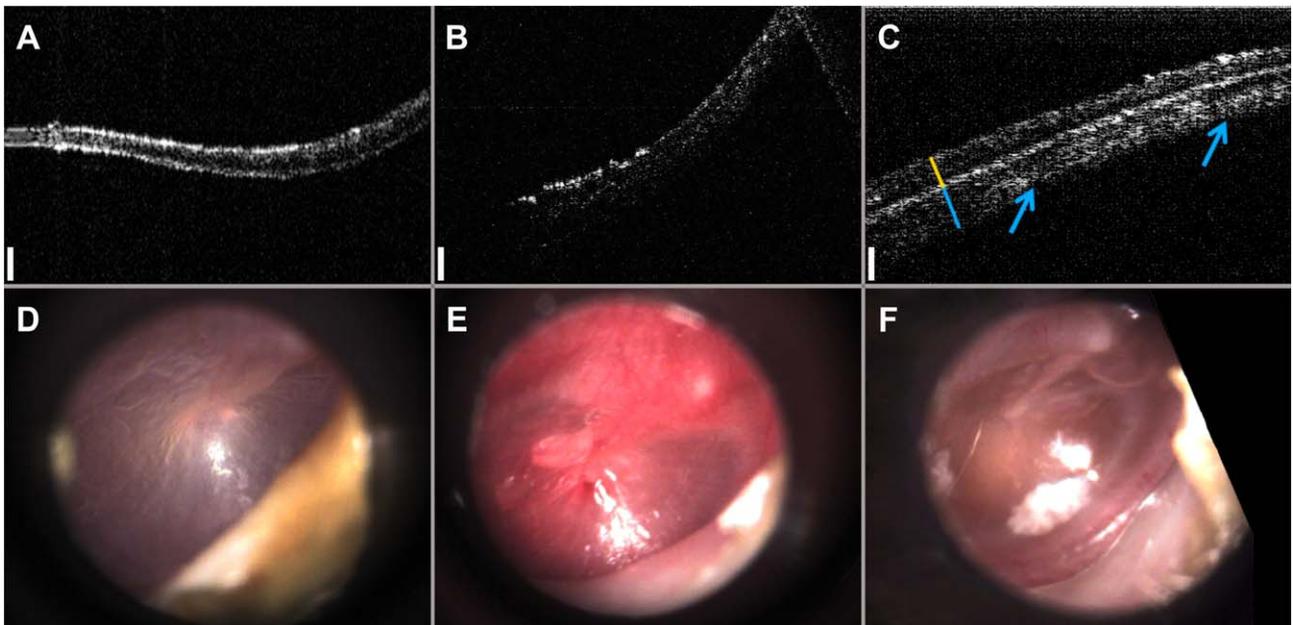
Fig. 2. Representative depth-resolved cross-sectional OCT images: (A) normal, (B) acute OM, (C) chronic OM, and representative en face images from a commercial video otoscope: (D) normal, (E) acute OM, (F) chronic OM. Data from OCT images (A–C) enables quantitative distinction between infection types. Yellow and blue lines in (C) denote the location of the TM (yellow) and the biofilm (blue). Arrows highlight extent of biofilm across TM. Scale bars (white) represent 150 microns in depth. OCT images (A–C) are displayed on equal intensity scales to highlight the differences in optical scattering between each group. OCT = optical coherence tomography; OM = otitis media; TM = tympanic membrane.

Subject	Patient History	TM Thickness (µm)
Normal		
N1	Normal	116
N2	Normal	116
N3	Normal	100
N4	Normal	100
N5	Normal	74
N6	Normal	139
N7	Normal	148
N8	Normal	90
N9	Normal	100
N10	Normal	130
N11	Normal	60
N12	Normal	105
N13	Normal	98
Acute		
A1	Acute OM	211
A2	ET dysfunction, mild inflammation	215
A3	OM, serous effusion	194
A4	Acute OM, semipurulent effusion	175
A5	Acute OM, serous effusion	150
A6	Acute OM	115
A7	Acute OM, serous effusion, inflammation	115
A8	AOM, erythema	180
A9	AOM, bulging TM, erythema	140
A10	Persistent acute OM, erythema	190
A11	Otitis externa, acute OM, TM perforation	197
A12	Recurrent acute OM	200
Chronic		
C1	Chronic OM	230 (105)
C2	Chronic OM	230 (NA)
C3	Chronic OM	380 (120)
C4	Chronic OM	410 (109)
C5	Mucoid chronic OM, ET dysfunction	280 (79)
C6	Chronic OM	310 (90)
C7	Chronic OM	340 (150)
C8	Chronic OM	190 (75)
C9	Chronic OM	230 (81)

In the chronic OM group, the total thickness is listed first, with the TM-only thickness, if available, in parentheses.

AOM = acute; ET = Eustachian tube; NA = not available; OM = otitis media; TM = tympanic membrane.

image features corresponding to the different pathologies encountered during imaging. Figure 2A shows a cross-sectional OCT scan of a normal, healthy TM, with typical high-scattering depth-resolved features and a thickness of approximately 100 microns, and with a representative video still image of a normal, healthy TM in Figure 2D. A cross-sectional OCT scan of an acute TM is shown in Figure 2B, showing an increased thickness

when compared to the normal case, most likely due to inflammation. When displayed on the same intensity scale, tympanic membranes with acute OM also typically exhibited lower optical scattering on OCT, compared to the normal and chronic OM cases. Figure 2E shows a video image of an acute TM, which is bulging, erythematous, and injected. A cross-sectional OCT image of a chronic TM (yellow line) is shown in Figure 2C. Although the TM has largely returned to normal thickness and optical scattering, a large, thick accompanying biofilm (blue line/arrows) is present with a clear boundary defining each structure. These structures were identified based on the physical orientation of the handheld probe, where the top of the figure faces the ear canal (to exterior) and the bottom of the figure faces the middle ear cavity (to interior). Figure 2F shows a representative video image of the chronic ear infection.

Table I lists the participating pediatric subjects in the study, along with relevant clinical history and overall measured TM thickness. Figure 3 shows a study protocol schematic that highlights the differences between two approaches to detecting and diagnosing OM. Although the physician's diagnostic evaluation focuses on the qualitative appearances of the TM at the time of exam, the optical measurements allow for a quantitative measurement of the thickness of the TM and provides additional information not available through visual inspection. Whereas Figure 3 visually shows the normal, acute, and chronic (TM and associated biofilm) infection
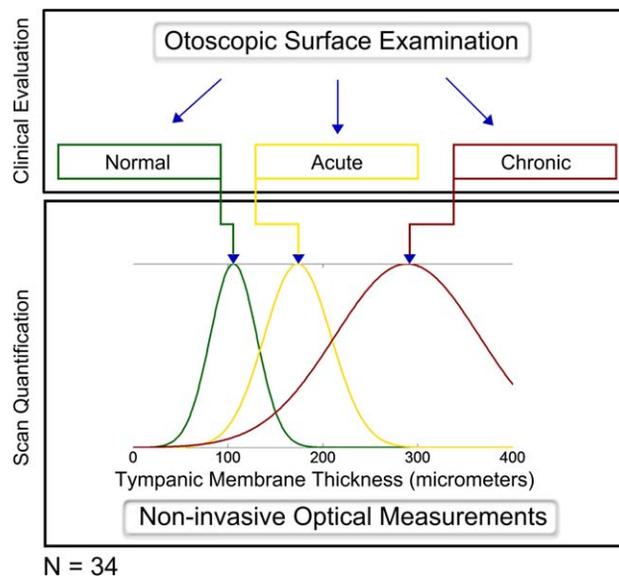

Fig. 3. Study protocol schematic. The physician first performs the needed clinical examinations to form an unbiased diagnostic opinion of the participant. While standard otoscopy exams provide qualitative information to the physician, depth-resolved optical measurements quantify the status of the middle ear. OCT scans are then acquired and processed, quantitatively calculating a value for the thickness of the TM. The values reported for the mean and standard deviation of each subgroup, as shown in Figure 4, were used to create these normalized distributions. (Note: Chronic TM-only group not shown.) OCT = optical coherence tomography; TM = tympanic membrane. [Color figure can be viewed in the online issue, which is available at www.laryngoscope.com.]
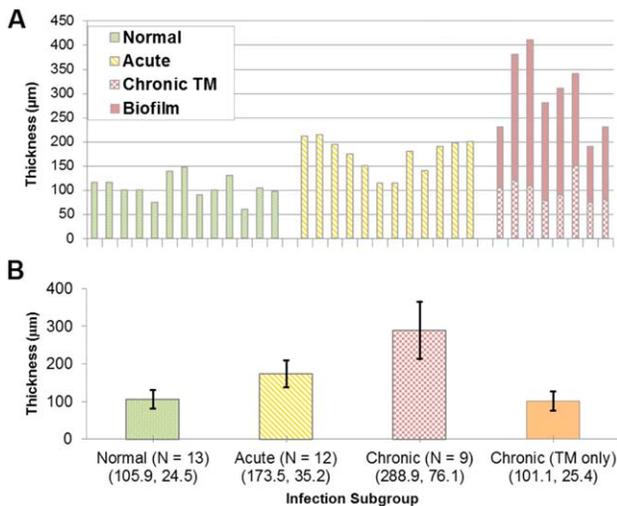
Fig. 4. Analysis of TM thickness between diagnostic groups. (A) Histogram of TM thickness. The chronic OM group has been subdivided to show thickness of the TM and biofilm. (B) Measured average thickness and statistical analysis presented by group. Mean and standard deviation (error bars) of thickness measurements in micrometers. TM = tympanic membrane. [Color figure can be viewed in the online issue, which is available at www.laryngoscope.com.]

groups as a normalized distributions based on the mean experimental data, Figure 4 shows the quantitative capabilities of this method. In Figure 4A, the chronic OM group is separated into TM-only thickness and biofilm thickness, whereas the composite represents total thickness. There is a clear trend of increasing overall thickness when comparing normal and chronic infections. Mean and standard deviation (SD) values for each group (normal, acute, chronic, and chronic TM-only) are displayed in Figure 4B.

The results from the relevant statistical calculations are shown in Table II. Each comparison shows statistically significant differences, indicating distinct groupings between infection types in this dataset. Statistical power calculations were performed for this currently presented set of pediatric data, but they were omitted from Table II. The means and SDs of the different groups are separated, completely in some instances; therefore, the power for most comparisons is near 1. Similar statistical calculations were performed when only considering the TM thickness (excluding the biofilm

thickness in the chronic OM infection group). These results show that whereas the chronic TM-only group is statistically different from the acute group, it is not statistically different from the normal group. This is somewhat unexpected; further studies are needed to investigate the mechanisms for why the chronic TM returns to a more normal baseline value, even in the presence of an adjacent biofilm in the middle ear.

DISCUSSION

A noninvasive, real-time, quantitative thickness measurement of the TM is demonstrated with OCT in normal, acute, and chronic cases of pediatric OM to quantify the state of infection in the middle ear. This technique can be used to assist in the clinical management of the disease and to provide further insight and understanding into the currently uncertain relationship between middle ear infection and biofilm formation. It is not possible to obtain this information with current clinical otoscopy methods, which rely mostly on subjective and qualitative diagnostic factors. The overall thickness of the TM and the presence of a biofilm are shown to be important indicators of infection and together are presented here as a new metrics to diagnose and monitor OM.

The analysis of this experimental data is inherently linked to understanding the optical scattering properties of the tissue. In general, the optical scattering properties of the TM correlate well with the stage of infection. It is expected that normal TMs will appear thin, with a thickness of approximately 100 micrometers, and have relatively strong, uniform scattering throughout the structure. When an acute infection is present, the TM is significantly thickened when compared to a normal TM and has a lower scattering signal as a result of a substantial inflammatory response, typically attributed to *Streptococcus pneumoniae*.[33] When inflamed, there will be an increase in interstitial fluid in the TM, which will physically separate or dilute scattering particles within the tissue. This will reduce the intensity of the backscattered light, making the tissue features less bright on the OCT image.

In chronic OM, where a biofilm is present, the optical scattering of the TM appears to return to a profile similar to the normal case. Similarly, even though the overall thickness increased significantly in chronic cases, the TM thickness (disregarding the associated biofilm) had largely returned to normal values. The presence of the additional scattering microstructure attributed to a middle-ear bacterial biofilm and affixed behind the TM was found in 89% (8/9) of chronic OM infections in this study. It should be noted that the ninth case had no discrete visible boundary between the TM and biofilm, but had a total thickness comparable to the other chronic OM cases. In this case, it is likely that the indices of refraction between the biofilm and TM were similar, making the boundary between them less detectable with OCT. In general, data from this current pediatric study and our previous adult clinical study[32] show similar thicknesses for normal TMs and for TMs with biofilms in subjects with chronic OM. This study presents new

TABLE II.
Statistical Results Between Normal, Acute OM, and Chronic OM Groups.

Comparison Group	t Value	P Value
Normal and acute	5.53	< 0.001
Normal and chronic	6.97	< 0.001
Acute and chronic	4.22	0.0016
Chronic (TM only) and normal	0.42	0.68
Chronic (TM only) and acute	5.33	< 0.001

OM = otitis media; TM = tympanic membrane.

findings from pediatric subjects with acute OM as well as further statistical analysis and comparison within the pediatric population.

The changes to the thickness of the TM and the presence or absence of a biofilm highlight the immune response mechanisms that occur during infection. However, the precise mechanism and cause by which the changes in TM thickness occur are still unclear. It is known that this persistent exposure to a bacterial infection or associated particulates results in an increase in the number of mucin-producing goblet cells in the middle ear mucosa,[34] which contributes to biofilm formation and persistence—and predictably the source of the clinically coined term *glue ear*. The embedded bacteria within the biofilm exist in a metabolically quieter state and contribute a much lower-level persistent exposure than planktonic bacteria. The resulting response from a persistent low-level exposure to pathogenic material is perhaps related to a tolerance mechanism to the infection[35] and may prepare the tissue to better withstand additional insult. The visible biofilm structure in the images presented here is potentially an indirect observation of the metaplastic changes that occur as a result of this infection process. The different levels of toxin loads produced by bacteria in planktonic or biofilm form in acute and chronic cases may influence the visible thickness changes to some degree. Considering that a biofilm can evade detection by the host immune system through various mechanisms,[13] including the ability to inhibit proinflammatory responses in tissue,[36] it may be that a lack of immune response is the cause. Overall, the underlying mechanisms in the ear that occur in short-term and chronic infections require further study and investigation.

There are several limitations to the collected data that must be addressed. First, our system was not configured to record the exact scan position information from different regions of the TM. However, the majority of data was collected near the light reflex because this was the most readily identifiable portion of the TM and the region that produced the brightest OCT signal. Therefore, the reported thickness measurements should be considered as an average from this region of the TM. The influx of additional cells, water, and blood due to inflammation present in acute OM will slightly alter the refractive index of the TM tissue, which will result in a small error in the measured thickness. Given that the refractive index of biological tissues varies by less than 10%, this thickness measurement due to changes in refractive index alone is also expected to be less than 10%. To account for the large differences in TM thickness observed in this study, the refractive index of an acute TM would need to be significantly higher (approximately 2.36) to solely account for this total increase in thickness. Therefore, the change in measured thickness of the TM is most likely due to a physically thicker TM, not solely a refractive index change due to inflammation. Ongoing research is also investigating the optical refractive indices of various species of bacteria in biofilms at different stages of growth.

In this study, the OCT system was limited to cross-sectional scans of the TM roughly 2 mm in depth and 2 to 3 mm in the transverse dimension. This was sufficient for extracting accurate thickness measurements. In the future, wider-field three-dimensional (3-D) scans of the TM will be used to fully account for any spatial variations across the TM. This may be most relevant in some early chronic OM cases for whom biofilm microstructure may be nonuniform or patchy and distributed randomly across the TM and middle ear.

In the future, longitudinal studies will track individual subjects throughout the management of this disease (from initial presentation of acute OM, during antibiotic treatment, in chronic OM, and after placement of tympanostomy tubes) to comprehensively follow these physiological changes and directly correlate them with the changing optical properties and OCT image features. Furthermore, these studies will attempt to provide a deeper understanding of the relationship between changes to tissue with infection as well as long-term tolerance strategies of the middle ear in chronic OM, and perhaps it will clarify the relationship between changes in thickness to the TM with immune response to infection. With the information from both the physical and otoscopic exams alongside these new additional quantitative metrics, physicians may be able to develop a more effective and individualized treatment plan for the patient.

Although quantitative baseline results are presented here, future prospective studies will be able to evaluate the treatment outcomes of different treatment plans based on the new information that OCT can provide of the TM and any associated biofilm. For example, ongoing studies seek to observe how a middle ear effusion or biofilm may respond to different courses of antibiotics or how a chronic TM and biofilm may resolve after a myringotomy procedure.

The device will be evaluated based on the outcomes of these and other future studies on its potential to provide physicians with more comprehensive information about the middle-ear status, which can be used to implement the most appropriate and effective treatment strategy to treat the infection. In the future, new system modifications will also be implemented for extended depth-ranging and 3-D volumetric imaging that can provide a view throughout the entire middle-ear cavity in vivo, encompassing the TM, any biofilm or effusion, and the middle ear mucosa to observe these structures and changes simultaneously.

CONCLUSION

This study presents a noninvasive and quantitative method to measure the in vivo thickness of the human TM, to identify middle-ear biofilms, and collectively to potentially help differentiate types of OM. Future investigations are needed to clarify which mechanisms are responsible for the observed decrease in chronic TM thicknesses toward relatively normal values. With the additional quantitative image-based diagnostic information provided by our imaging system, decisions for determining the appropriate patient care could be supported with quantitative findings and monitored over time

throughout the treatment period. Future studies, in addition to following individual subjects longitudinally, will prospectively evaluate the use of this technology in treatment outcomes. This technology provides physicians with the new ability to noninvasively quantify the thickness of the in vivo TM and objectively identify the presence or absence of a middle-ear biofilm.

BIBLIOGRAPHY

1. Lieberthal AS, Carroll AE, Chonmaitree T, et al. The diagnosis and management of acute otitis media. *Pediatrics* 2013;131:964–999.
2. Linsk R, Blackwood A, Cooke J, Harrison V, Lesperance M, Hildebrandt HM. University of Michigan Health System. *Guidelines for clinical care. Otitis media*. Ann Arbor, MI: Regents of the University of Michigan; updated 2002 May. Available at: http://www.med.umich.edu/1info/FHP/practice guides/om/OM.pdf. Accessed January 9, 2015.
3. Shekelle P, Takata G, Chan LS, et al. Diagnosis, natural history, and late effects of otitis media with effusion. *Evid Rep Technol Assess (Summ)* 2002;55:1–5.
4. Jones WS, Kaleida PH. How helpful is pneumatic otoscopy in improving diagnostic accuracy? *Pediatrics* 2003;112:510–513.
5. Morris E, Kesser BW, Peirce-Cottler S, Keeley M. Development and validation of a novel ear simulator to teach pneumatic otoscopy. *Simul Healthc* 2012;7:22–26.
6. Vaile L WT, Waddell A, Taylor GJ. Interventions for ear discharge associated with grommets (ventilation tubes). *Cochrane Database Syst Rev* 2006;(2):CD001933.
7. Kelley R. Where can $700 billion in waste be cut annually from the US healthcare system? Ann Arbor, MI: *Thomson-Reuters*. October 2009. Available at: http://www.ncrponline.org/PDFs/2009/Thomson_Reuters_White_Paper_on_Healthcare_Waste.pdf. Accessed May 25, 2014.
8. American Academy of Pediatrics Subcommittee on Management of Acute Otitis Media. Diagnosis and management of acute otitis media. *Pediatrics* 2004;113:1451–1465.
9. Post JC. Direct evidence of bacterial biofilms in otitis media. *Laryngoscope* 2001;111:2083–2094.
10. Bakaletz LO. Bacterial biofilms in otitis media: evidence and relevance. *Pediatr Infect Dis J* 2007;26:17–19.
11. Musk Jr DJ, Hergenrother PJ. Chemical countermeasures for the control of bacterial biofilms: effective compounds and promising targets. *Curr Med Chem* 2006;13:2163–2177.
12. Rhoads DD, Wolcott RD, Percival SL. Biofilms in wounds: management strategies. *J Wound Care* 2008;17:502–508.
13. Fedtke I, Gotz F, Peschel A. Bacterial evasion of innate host defenses–the Staphylococcus aureus lesson. *Int J Med Microbiol* 2004;294:189–194.
14. Ehrlich GD, Veeh R, Wang X, et al. Mucosal biofilm formation on middle-ear mucosa in the chinchilla model of otitis media. *Journal of the American Medical Association.* 2002;287(13):1710–1715.
15. Hall-Stoodley L, Hu FZ, Gieseke A, et al. Direct detection of bacterial biofilms on the middle-ear mucosa of children with chronic otitis media. *JAMA* 2006;296:202–211.
16. Kania RE, Lamers GEM, Vonk MJ, et al. Characterization of mucosal biofilms on human adenoid tissues. *Laryngoscope* 2008;118:128–134.
17. Hoa M, Syamal M, Schaeffer MA, Sachdeva L, Berk R, Coticchia J. Biofilms and chronic otitis media: an initial exploration into the role of biofilms in the pathogenesis of chronic otitis media. *Am J Otolaryngol* 2010;31:241–245.
18. Nistico L, Kreft R, Gieseke A, et al. Adenoid reservoir for pathogenic biofilm bacteria. *J Clin Microbiol* 2011;49:1411–1420.
19. Winther B, Gross BC, Hendley JO, Early SV. Location of bacterial biofilm in the mucus overlying the adenoid by light microscopy. *Arch Otolaryngol Head Neck Surg* 2009;135:1239–1245.
20. Psaltis AJ, Weitzel EK, Ha KR, Wormald P-J. The effect of bacterial biofilms on postsinus surgical outcomes. *Am J Rhinol* 2008;22:1–6.
21. Prince AA, Steiger JD, Khalid AN, et al. Prevalence of biofilm-forming bacteria in chronic rhinosinusitis. *Am J Rhinol* 2008;22:239–245.
22. Chen F, Zha D, Fridberger A, et al. A differentially amplified motion in the ear for near-threshold sound detection. *Nature Neurosci* 2011;14: 770–774.
23. Subhash HM, Davila V, Sun H, Nguyen-Huynh AT, Nuttall AL, Wang RK. Volumetric *in vivo* imaging of intracochlear microstructures in mice by high-speed spectral domain optical coherence tomography. *J Biomed Opt* 2010;15:036024.
24. Hamid R, Rubinstein M, EC Wu, Naemi K. Optical coherence tomography of cholesteatoma. *Otol Neurotol* 2010;31:932–935.
25. Pitris C, Saunders KT, Fujimoto JG, Brezinski ME. High-resolution imaging of the middle ear with optical coherence tomography: a feasibility study. *Arch Otolaryngol Head Neck Surg* 2001;127:637–642.
26. Van der Jeught S, Dirckx JJ, Aerts JR, Bradu A, Podoleanu AG, Buytaert JA. Full-field thickness distribution of human tympanic membrane obtained with optical coherence tomography. *J Assoc Res Otolaryngol* 2013;14:483–494.
27. Xi C, Marks D, Schlachter S, Luo W, Boppart SA. High-resolution three-dimensional imaging of biofilm development using optical coherence tomography. *J Biomed Opt* 2006;11:034001.
28. Chaney EJ, Nguyen CT, Boppart SA. Novel method for non-invasive induction of a middle-ear biofilm in the rat. *Vaccine* 2011;29:1628–1633.
29. Nguyen CT, Tu H, Chaney EJ, Stewart CN, Boppart SA. Non-invasive optical interferometry for the assessment of biofilm growth in the middle ear. *Biomed Opt Express* 2010;1:1104–1116.
30. Jung W, Kim J, Jeon M, Chaney EJ, Stewart CN, Boppart SA. Handheld optical coherence tomography scanner for primary care diagnostics. *IEEE Trans Biomed Eng* 2011;58:741–744.
31. Shelton RL, Jung W, Sayegh SI, McCormick DT, Kim J, Boppart SA. Optical coherence tomography for advanced screening in the primary care office. *J Biophotonics* 2014;7:525–533.
32. Nguyen CT, Jung W, Kim J, et al. Noninvasive in vivo optical detection of biofilm in the human middle ear. *Proc Natl Acad Sci U S A* 2012;109: 9529–9535.
33. Liu K, Kaur R, Almudevar A, Pichichero ME. Higher serum levels of Interleukin 10 occur at onset of acute otitis media caused by Streptococcus pneumoniae compared to Haemophilus influenzae and Moraxella catarrhalis. *Laryngoscope* 2013;123:1500–1505.
34. Lin J, Tsuboi Y, Rimell F, et al. Expression of mucins in mucoid otitis media. *J Assoc Res Otolaryngol* 2003;4:384–393.
35. Medzhitov R, Schneider DS, Soares MP. Disease tolerance as a defense strategy. *Science* 2012;335:936–941.
36. Thurlow LR, Hanke ML, Fritz T, et al. Staphylococcus aureus biofilms prevent macrophage phagocytosis and attenuate inflammation *in vivo*. *J Immunol* 2011;186:6585–6596.